

**SYNTHESIS, CHARACTERIZATION AND OPTIMIZATION OF  
NANOCOMPOSITE SCAFFOLD USING POLY LACTIDE/MULTI-  
WALLED CARBON NANOTUBES**

**by**

**HASSAN ADELI JELODAR**

**Thesis submitted in fulfillment of the requirements**

**for the degree of**

**Master of Science**

**May 2011**

## ACKNOWLEDGEMENT

**In the name of Allah, the Most Beneficent, the Most Merciful.**

I wish to express my gratitude to my beloved parents, brother and sister for their encouragement, support and patience throughout my life and education.

I would like to express my sincere and profound appreciation to my dedicated supervisor, Assoc. Prof. Dr. Sharif Hussein Sharif Zein for his excellent, generous and continuous guidance throughout my research. There are no words to articulate how grateful I am to have had the honour and pleasure to work under his supervision. His professionalism, experience, advice, constructive criticism and unconditional support have provided me opportunity to be success in my project. Besides, I would also like to extend my gratitude to my co-supervisor, Prof. Abdul Latif Ahmad. In addition I would like to thank my field supervisors, Dr. Tan soon Huat and Assoc. Prof. Dr. Hazizan Md Akil for their effort spent in guiding me throughout my study.

I would like to thank the administrative staff of School of Chemical Engineering at Universiti Sains Malaysia, especially our respected Dean, Prof. Azlina Harun @ Kamaruddin, Deputy Dean and all the technicians for their support during my research. I would also like to thank the financial support (Research Assistantship) during my research which was provided by the Universiti Sains Malaysia.

I would like to acknowledge and thank all of my friends, Mr.Rezaei, Mr.Mazaheri, Mr.Hassani and others for their help, support and significant contributions during my study.

## TABLE OF CONTENTS

	Page
ACKNOWLEDGEMENT .....	ii
TABLE OF CONTENTS .....	iii
LIST OF TABLES .....	vii
LIST OF FIGURES .....	ix
LIST OF SYMBOLS .....	xv
ABSTRAK .....	xvi
ABSTRACT .....	xviii
CHAPTER 1 - INTRODUCTION .....	1
1.1 Introduction .....	1
1.2 Problem Statement .....	7
1.3 Objectives of research .....	8
1.4 Outline of the thesis .....	9
CHAPTER 2 - LITERATURE REVIEW .....	11
2.1 Polylactide/poly(lactic acid).....	11
2.1.1 Introduction .....	11
2.1.2 Synthesis, Mechanisms, and Commercial Production .....	<b>Error! Bookmark not defined.</b>
2.1.3 PLA Properties .....	<b>Error! Bookmark not defined.</b>
2.1.4 PLA Modifications .....	14
2.1.5 Degradation .....	17
2.1.6 PLA applications .....	18
2.2 Carbon nanotubes (CNTs) .....	20
2.2.1 Synthesis of CNTs.....	20

2.2.2 Mechanical Properties of CNTs .....	24
2.2.3 Thermo-elastic Properties of CNTs.....	26
2.2.4 Thermal Conductivity of CNTs.....	27
2.2.5 Alignment of Nanotubes in the Composites.....	29
2.3 Biomaterial classifications .....	30
2.3.1 Ceramic biomaterials.....	31
2.3.2 Metallic biomaterials .....	32
2.3.3 Polymeric biomaterials.....	33
2.3.4 Composite biomaterials .....	35
2.4 Scaffold .....	36
2.4.1 Scaffolds application and requirements.....	36
2.4.2 Scaffold Fabrication .....	37
2.5 Statistical Analysis of Data .....	43
2.5.1 Design of Experiments (DOE) .....	43
2.5.2 Response Surface Methodology (RSM).....	44
2.5.3 Central Composite Design (CCD).....	45
2.5.4 Model Fitting and Statistical Analysis .....	47
<b>CHAPTER 3 - MATERIALS AND METHODS .....</b>	<b>49</b>
3.1 Materials.....	49
3.2 Experimental method .....	49
3.2.1 Scaffold preparation by freeze extraction method.....	49
3.3 Characterization .....	52
3.3.1 Mechanical test.....	52
3.3.2 Differential scanning calorimeter (DSC).....	52
3.3.3 Thermogravimetric analysis (TGA).....	52

3.3.4 Fourier-transform infrared spectroscopy (FTIR).....	52
3.3.5 Density.....	53
3.3.6 Scanning electron microscopy (SEM).....	53
3.3.7 Porosity of scaffolds .....	53
3.3.8 Swelling degree of scaffolds .....	54
3.3.9 In vitro degradation of the scaffolds.....	54
3.4 Optimization studies by Design of Experiment (DOE) .....	55
3.4.1 Response Surface Methodology (RSM).....	56
3.4.2 Experimental data repeatability .....	59
<b>CHAPTER 4 - RESULTS AND DISCUSSIONS .....</b>	<b>60</b>
4.1 Scaffold characterization.....	60
4.1.1 Mechanical properties of the scaffolds.....	60
4.1.2 Thermal properties of the scaffolds.....	61
4.1.3 FTIR analysis of the scaffolds.....	63
4.1.4 Morphological properties of the scaffolds before degradation.....	65
4.1.5 Porosity, Pore size and density of the scaffolds .....	68
4.1.6 Swelling degree of the scaffolds.....	71
4.1.7 In vitro degradation of the scaffolds (weight loss).....	72
4.1.8 Morphological properties of the scaffolds after degradation .....	73
4.2 Optimization studies .....	77
4.2.1 The design of experiments analysis and model fitting .....	77
4.2.2 Numerical optimization .....	112
<b>CHAPTER 5 - CONCLUSIONS.....</b>	<b>119</b>
5.1 Conclusions.....	119
5.2 Suggestions for further studies.....	121

<b>REFERENCES</b> .....	122
<b>LIST OF PUBLICATIONS</b> .....	131

## LIST OF TABLES

	Page
Table 2. 1 Thermal properties of PLA(Jamshidi <i>et al.</i> , 1988; Ikada and Tsuji, 2000; Tsuji, Miyase et al., 2005).....	12
Table 2. 2 Physical properties of PLA (Shogren, 1997; Tsuji and Muramatsu, 2001; Biresaw and Carriere, 2002).....	13
Table 2. 3 Applications of PLA and their copolymer (Ikada and Tsuji, 2000).....	18
Table 2. 4 Commercial applications of PLA (Ikada and Tsuji, 2000) .....	20
Table 2. 5 Materials for Use in the Body (Park and Bronzino, 2003) .....	31
Table 2. 6 Biomedical applications of polymeric biomaterials.....	34
Table 3. 1 Experimental range and levels of the respective independent variables...	56
Table 3. 2 Experimental matrix for coded and actual value of the respective independent variables.....	57
Table 4. 1 Pore size and porosity of pure PLLA, 0.5 wt % MWCNT/PLLA, 1 wt % MWCNT/PLLA, 3 wt % MWCNT/PLLA and 5 wt % MWCNT/PLLA scaffolds .....	69
Table 4. 2 The experimental design and actual response of modulus, strength and elongation.....	78
Table 4. 3 The ANOVA for the modulus (Unreduced models).....	79
Table 4. 4 The ANOVA for the modulus (reduced models).....	81
Table 4. 5 Statistical parameters of the reduced model equation as obtained from the ANOVA models for the modulus .....	82
Table 4. 6 ANOVA for the strength (Unreduced models).....	91
Table 4. 7 The ANOVA for the strength (reduced models).....	92

Table 4. 8 Statistical parameters of the reduced model equation as obtained from the ANOVA models for the strength .....	94
Table 4. 9 The ANOVA for the elongation (Unreduced models).....	101
Table 4. 10 The ANOVA for the elongation (reduced models).....	102
Table 4. 11 Statistical parameters of the reduced model equation as obtained from the ANOVA models for the elongation .....	104
Table 4. 12 Constraints of each variable for the numerical optimization of the modulus .....	112
Table 4. 13 Optimum conditions to obtain the maximum modulus.....	113
Table 4. 14 Constraints of each variable for the numerical optimization of the strength.....	113
Table 4. 15 Optimum conditions to obtain the maximum strength.....	114
Table 4. 16 Constraints of each variable for the numerical optimization of the elongation.....	114
Table 4. 17 Optimum conditions to obtain the maximum elongation.....	115
Table 4. 18 Constraints of each variable for the numerical optimization of the modulus, strength and elongation.....	116
Table 4. 19 Optimum conditions for maximum modulus, strength and elongation	116
Table 4. 20 Results of validate experiments conducted at the optimum conditions as obtained from DOE for modulus.....	117
Table 4. 21 Results of validate experiments conducted at the optimum conditions as obtained from DOE for strength.....	117
Table 4. 22 Results of validate experiments conducted at the optimum conditions as obtained from DOE for elongation.....	118

## LIST OF FIGURES

	Page
Figure 2. 1 Cyclic dimerization by condensation of L-, and D-lactic acids into L-, D-, and <i>meso</i> -lactides. ....	<b>Error! Bookmark not defined.</b>
Figure 2. 2 Molecular structures of other lactones and aliphatic polyesters .....	<b>Error! Bookmark not defined.</b>
Figure 2. 3 Synthesis of lactic acid and poly(lactic acid) (Vink <i>et al.</i> , 2003; Mecking, 2004) .....	<b>Error! Bookmark not defined.</b>
Figure 2. 4 Polymerization of lactide to PLA using R-OH/Sn(Oct) <sub>2</sub> initiator/catalyst system.....	<b>Error! Bookmark not defined.</b>
Figure 2. 5 Activated monomer mechanism for ROP of lactides using Sn(Oct) <sub>2</sub> .....	<b>Error! Bookmark not defined.</b>
Figure 2. 6 Tin (II) alkoxide complex initiated ROP of lactides using Sn(Oct) <sub>2</sub> . .....	<b>Error! Bookmark not defined.</b>
Figure 2. 7 Cationic polymerization mechanism for the Sn(Oct) <sub>2</sub> /lactone system as .....	<b>Error! Bookmark not defined.</b>
Figure 2. 8 Cationic polymerization mechanism for the Sn(Oct) <sub>2</sub> /lactide system as .....	<b>Error! Bookmark not defined.</b>
Figure 2. 9 Synthesis of oligoethylene-end-capped PLA .....	15
Figure 2. 10 Hydrolysis mechanism for PLA [1].....	18
Figure 2. 11 Schematic diagram showing how a hexagonal sheet of graphene is “rolled” to form a CNTs.....	22
Figure 2. 12 Central composite design layout, with replicated center points, factorial and axial points spatially distributed (Cho and Zoh, 2007) .....	46
Figure 3. 1 Solvent extraction method .....	50

Figure 3. 2 Schematic diagrams of the experimental procedures .....	51
Figure 4. 1 Tensile strength, modulus and elongation results of pure PLLA, 0.5 wt % MWCNT/PLLA, 1 wt % MWCNT/PLLA, 3 wt % MWCNT/PLLA and 5 wt % MWCNT/PLLA scaffolds.....	61
Figure 4. 2 Variation of decomposition temperature and weight loss of pure PLLA, 0.5 wt % MWCNT/PLLA, 1 wt % MWCNT/PLLA, 3 wt % MWCNT/PLLA and 5 wt % MWCNT/PLLA scaffolds .....	62
Figure 4. 3 Variation of melting point temperature ( $T_m$ ) and glass transition temperature ( $T_g$ ) of pure PLLA, 0.5 wt % MWCNT/PLLA, 1 wt % MWCNT/PLLA, 3 wt % MWCNT/PLLA and 5 wt % MWCNT/PLLA scaffolds .....	63
Figure 4. 4 FTIR spectra of (a) pure PLLA, (b) MWCNTs, (c) 0.5 wt % MWCNT/PLLA, (d) 1 wt % MWCNT/PLLA, (e) 3 wt % MWCNT/PLLA and (f) 5 wt % MWCNT/PLLA scaffolds .....	64
Figure 4. 5 Cross-sectional SEM images of the (a) pure PLLA, (b) 0.5 wt % MWCNT/PLLA, (c) 1 wt % MWCNT/PLLA, (d) 3 wt % MWCNT/PLLA and (e) 5 wt % MWCNT/PLLA scaffolds.....	66
Figure 4. 6 Porosity and bulk density of pure PLLA, 0.5 wt % MWCNT/PLLA, 1 wt % MWCNT/PLLA, 3 wt % MWCNT/PLLA and 5 wt % MWCNT/PLLA scaffolds.....	70
Figure 4. 7 Effect of MWCNT loading on the swelling degree of pure PLLA, 0.5 wt % MWCNT/PLLA, 1 wt % MWCNT/PLLA, 3 wt % MWCNT/PLLA and 5 wt % MWCNT/PLLA scaffolds.....	71

Figure 4. 8 Weight loss resulting from in vitro degradation of (a) pure PLLA, (b) 0.5 wt % MWCNT/PLLA, (c) 1 wt % MWCNT/PLLA, (d) 3 wt % MWCNT/PLLA and (e) 5 wt % MWCNT/PLLA scaffolds .....	73
Figure 4. 9 Cross-sectional SEM images of the scaffolds after in vitro degradation: (a) pure PLLA, (b) 0.5 wt % MWCNT/PLLA, (c) 1 wt % MWCNT/PLLA, (d) 3 wt % MWCNT/PLLA and (e) 5 wt % MWCNT/PLLA .....	74
Figure 4. 10 Comparison between the predicted and actual experiment values for the modulus .....	83
Figure 4. 11 The main effect plots of the model terms on the Modulus (a) ratio of PLLA/(PLLA+MWCNT) and (b) freezing time .....	85
Figure 4. 12 The interaction between the solvent amount ( $X_2$ ) and ratio of PLA/(PLA+MWCNT) ( $X_1$ ) on the modulus (a) 2D plot (b) 3D plot.....	99
Figure 4. 13 The 3D plot representing the interaction between the freezing time ( $X_3$ ) and solvent amount ( $X_2$ ) on the modulus (a) 2D plot (b) 3D plot.....	88
Figure 4. 14 The interaction between the immersing time ( $X_4$ ) and solvent amount ( $X_2$ ) on the modulus (a) 2D plot and (b) 3D plot .....	89
Figure 4. 15 Comparison between the predicted and actual experiment values for the strength .....	95
Figure 4. 16 The main effect plots of the model terms for the strength (a) ratio of PLLA/(PLLA+MWCNT) and (b) immersing time.....	96
Figure 4. 17 The interaction between the freezing time( $X_3$ ), ratio of PLA/(PLA+MWCNT) ( $X_1$ ) and immersing time ( $X_4$ ) on the strength (a) 2D plot and (b) 3D plot.....	98

Figure 4. 18 The interaction between the freezing time ( $X_3$ ) and immersing time ( $X_4$ ) on the strength (a) 2D plot and (b) 3D plot.....	99
Figure 4. 19 Comparison between the predicted and actual experimnet values for the elongation .....	105
Figure 4. 20 The main effect plots of the model terms for the elongation (a) ratio of PLLA/(PLLA+MWCNT), (b) solvent amount (c) freezing time and (d) immersing time.....	106
Figure 4. 21 The interaction between the freezing time, ratio of PLA/(PLA+MWCNT) ( $X_1$ ) and solvent amount ( $X_2$ ) on the elongation (a) 2D plot and (b) 3D plot.....	109
Figure 4. 22 The interaction between the freezing time ( $X_3$ ) and immersing time ( $X_4$ ) on the elongation (a) 2D plot and (b) 3D surface.....	110

## LIST OF ABBREVIATIONS

ANOVA	Analysis of variance
ASTM	American Society of Testing and Materials
ATR-IR	Attenuated total reflectance infrared
$\beta$ -BL	$\beta$ - butyrolactone
CCD	Central composite design
CVD	chemical vapor decomposition
CNTs	Carbon nanotubes
CTE	Coefficient of thermal expansion
DOE	Design of experiments
DSC	Differential scanning calorimeter
DWNT	double-wall nanotubes
DXO	1,5-dioxepan-2-one
$\epsilon$ -CL	$\epsilon$ -caprolactone
FTIR	Fourier-transform infrared spectroscopy
F-value	Fisher's F value
KBr	Potassium bromide
MWCNTs	Multiwall carbon nanotubes
PCL	Poly ( $\epsilon$ -caprolactone)
PBS	Phosphate buffer saline
PBPs	Petroleum-based polymers
PDI	polydispersity index
PE	Polyethylene
PEG	Poly(ethylene glycol)

PEO	Poly(ethylene oxide)
PP	Polypropylene
PS	Polystyrene
PGA	Polyglycolide or Polyglycolic acid
PLA	Poly lactide
PLLA	Poly (L-lactide acid)
P(LLA-co-CL)	Poly (lactic-co- $\epsilon$ -caprolactone)
PLGA	Poly (lactic-co-glycolic acid)
PMMA	Poly(methyl methacrylate)
P-value	Probability value
ROP	Ring-opening polymerization
RSM	Response surface methodology
Sn(Oct) <sub>2</sub>	Stannous octoate
SD	Standard deviations
SEM	Scanning electron microscope
SWCNTs	single-wall carbon nanotubes
TGA	Thermogravimetric analysis

## LIST OF SYMBOLS

g	gram
h	Hour
Hz	Hertz
KPa	Kilo Pascal
M <sub>n</sub>	Number average molecular weight
M <sub>s</sub>	mass of swollen scaffold
M <sub>d</sub>	dry scaffold
M <sub>w</sub>	Weight average molecular weight
M	Molar
MPa	Mega Pascal
min	Minute
nm	nanometer
T <sub>c</sub>	Cold crystallization temperature
T <sub>g</sub>	Glass transition temperature
T <sub>m</sub>	Melting temperature
V	volume of the obtained scaffold
V <sub>p</sub>	volume of polymer in scaffold
wt%	Weight percentage
μm	Micron meter
°C	Degree Centigrade
W <sub>d</sub>	surplus weight of scaffold after degradation
W <sub>i</sub>	initial weight of scaffold before degradation

**SINTESIS, PENCIRIAN DAN OPTIMASI SCAFFOLD KOMPOSIT NANO  
MENGUNAKAN LAKTIDA POLI LAKTIDE/ NANO TIUB KARBON  
BERDIN DING LAPISAN**

**ABSTRAK**

Poli (L-laktide) (PLLA) perancah telah banyak digunakan dalam kejuruteraan tisu dalam rangka untuk memperbaharui kulit, tulang, tulang rawan, ikatan sendi dan lain-lain. PLLA mempunyai kelebihan kebolehubaian biologi, kadar penguraian terkawal, sifat haba yang baik dan kesesuaian biologi. Ia dapat dihasilkan dari sumber yang diperbaharui, dan ia tidak beracun bagi manusia dan persekitaran. Walau bagaimanapun, sebahagian besar daripada perancah tiga dimensi (3D) dibuat dari PLLA secara relatif memiliki sifat mekanik lemah dan mereka tidak mampu memenuhi keperluan untuk aplikasi tertentu. Sebuah kaedah umum untuk meningkatkan sifat mekanik sesuatu matrik polimer adalah dengan menggabungkan pengisi ke dalam polimer sebagai agen penguat. Tiubnano karbon bermacam dinding (TNKBD) dianggap agen penguat unggul kerana sifat mereka yang unik. Gabungan TNKBD dalam matrik polimer mengarah kepada pembaikan sifat polimer yang luar biasa. Oleh itu, tujuan projek ini adalah untuk menyelidik sintesis, pencirian dan optimasi poli (L-laktida)/ tiubnano karbon bermacam dinding (PLLA / TNKBD) baru perancah berliang disediakan oleh kaedah pengekstrakan-beku untuk aplikasi kejuruteraan tisu. Beberapa teknik pencirian seperti mikroskop imbasan elektron (SEM), analisis termogravimetri (TGA), calorimeter imbasan perbezaan (DSC) dan analisis spektroskopi Fourier-transform inframerah (FTIR) digunakan untuk menilai sifat morfologi, haba, struktur dan mekanikal perancah. Perancah yang diperoleh menunjukkan penyebaran yang baik dan struktur berliang yang saling bersambungan

dengan lebih daripada 80% keliangan dan saiz liang rata-rata sekitar 40  $\mu\text{m}$  tersebar dalam saiz antara 50 dan 150  $\mu\text{m}$ . Sebagai hasil dari interaksi antara muka yang tinggi antara PLLA dan TNKBD, perancah telah mempamerkan peningkatan luar biasa pada sifat mekanik seperti modulus, kekuatan dan rentangan. Kajian penguraian invitro terhadap perancah dinilai dengan merendam perancah dalam penyangga fosfat salin (PBS) sehingga 24 minggu. Didapati bahawa penggabungan TNKBD dalam perancah PLLA telah menurunkan kadar penguraian invitro. Dalam rangka untuk memiliki proses pembelajaran yang sistematik, corak eksperimen (DOE) perkakasan lembut disatukan dengan metodologi permukaan tindakbalas (RSM) dan corak komposit pusat (CCD) digunakan untuk menyelidik hubungan modulus, kekuatan dan rentangan perancah dengan proses yang berbeza parameter, yang kemudiannya digunakan untuk proses pengoptimuman. Berdasarkan pengoptimuman tindakbalas bermacam, keadaan optimum untuk memiliki modulus maksimum (229.71 MPa), kekuatan (60.52 MPa) dan rentangan(10.72%) secara serentak diperoleh dengan penguatan 3.93% berat dari TNKBD, 157.62 ml kandungan pelarut, 5.10 jam tempoh pembekuan dan 2.81 hari tempoh rendaman.

**SYNTHESIS, CHARACTERIZATION AND OPTIMIZATION OF  
NANOCOMPOSITE SCAFFOLD USING POLY LACTIDE/MULTI-  
WALLED CARBON NANOTUBES**

**ABSTRACT**

Poly(L-lactide) (PLLA) scaffolds have been widely used in tissue engineering in order to regenerate the skin, bone, cartilage, ligament and etc. PLLA has the advantages of biodegradability, a controllable degradation rate, good thermal properties and biocompatibility. It can be produced from renewable resources, and it is nontoxic to humans and the environment. However, most of the three dimensional (3D) scaffolds made by PLLA have relatively poor mechanical properties and they are unable to meet the requirements for certain applications. A common method of improving the mechanical properties of a polymer matrix is to incorporate fillers into the polymer as a reinforcement agent. Multi-walled carbon nanotubes (MWCNTs) are considered to be an ideal reinforcing agent due to their unique properties. The incorporation of MWCNTs in a polymer matrix leads to remarkably improved properties of the polymer. Therefore, the aim of this project was to investigate the synthesis, characterization and optimization of the novel poly(L-lactide)/multi-walled carbon nanotube (PLLA/MWCNT) porous scaffolds prepared by the freeze-extraction method for tissue engineering application. Several characterization techniques such as scanning electron microscopy (SEM), thermogravimetric analysis (TGA), differential scanning calorimetry (DSC) and Fourier-transform infrared spectroscopy analysis (FTIR) were used to evaluate the morphological, thermal, structural and mechanical properties of the scaffolds. The obtained scaffolds showed well-distributed and interconnected porous structures with more than 80% porosity

and median pore size around 40  $\mu\text{m}$  distributed within a region between 50 and 150  $\mu\text{m}$  in size. As a result of high interfacial interaction between PLLA and the MWCNTs, the scaffolds exhibited remarkable improvements in mechanical properties such as modulus, strength and elongation. *In vitro* degradation studies of the scaffolds were assessed by immersing the scaffolds in phosphate buffered saline (PBS) for up to 24 weeks. It was found that the incorporation of MWCNTs in PLLA scaffolds decreased the rate of *in vitro* degradation. In order to have a systematic process study, design of experiment (DOE) software coupled with response surface methodology (RSM) and central composite design (CCD) was used to investigate the relation of the modulus, strength and elongation of the scaffolds with different process parameters, which were then used for the optimization process. Based on the multi responses optimization, the optimum conditions for having the maximum modulus (229.71 MPa), strength (60.52 MPa) and elongation (10.72 %) simultaneously was obtained with reinforcing 3.93 wt % of MWCNTs, 157.62 ml solvent content, 5.10 hr freezing hours and 2.81 days immersing time.

## CHAPTER 1

### INTRODUCTION

#### 1.1 Introduction

In the swiftly growing field of tissue engineering, novel biomaterials are being intensely examined. The use of polymeric biomaterials started in the 1940s during the Second World War (Castner and Ratner, 2002). Recent advances in polymeric biomaterials have been focused on tissue engineering towards solving problems of patients who have suffered tissue and organ loss or imperfection (Hu *et al.*, 2003). This is an indispensable step toward the application of scaffolds in tissue engineering. The development of polymeric biomaterials can be considered as an evolutionary improvement. A biomaterial is defined as a material intended to interface with biological systems to evaluate, treat, augment or replace any tissue, organ or function of the body (Williams, 1999). Reports on the applications of natural polymers as biomaterials date back thousands of years (Barbucci, 2002). Polymeric biomaterials are relatively easy to manufacture into products with various shapes, at reasonable cost, and with desirable mechanical and physical properties. However, the application of synthetic polymers to medicine is more or less a recent phenomenon.

Tissue engineering has emerged in the last decade of the 20th century as an alternative approach to circumvent the existent limitations in the current therapies. Many applications of tissue engineering which was intensively studied and reported include blood vessels (Vaz *et al.*, 2005), heart valves, bone, skin (Chen *et al.*, 2005) cartilage regeneration (Cohen *et al.*, 2003), nerves, liver and other organ systems

(Morita *et al.*, 2002). Other potential applications of tissue engineering include the replacement of worn and poorly functioning tissues; replacement of small caliber arteries, veins, coronary, and peripheral stents; replacement of the bladder and fallopian tube; and restoration of cells to produce necessary enzymes, hormones, and other bioactive products (Lanza *et al.*, 2007).

The principle of tissue engineering involves fabrication of new and functional living tissue using living cells, which are usually associated, in one way or another, with a matrix or scaffolding to guide tissue development. Thereby, tissue engineering has the potential to produce a supply of immunologically tolerant ‘artificial’ organ and tissue substitutes that can grow with the patient. This should lead to a permanent solution to the damaged organ or tissue without the need for supplementary therapies, thus making it a cost-effective treatment in the long term (Patrick Jr *et al.*, 1998; Hutmacher, 2000). Hence, many natural and synthetic polymeric biomaterials and their hybrid matrices have been developed to be used in tissue engineering applications (Agrawal and Ray, 2001; Li and Tuan, 2005 ; Smith *et al.*, 2009).

Bio based and biodegradable materials are the most well-known terms among the researchers in the world nowadays due to their sustainability and biodegradability (Stevens, 2002). The term “bio based polymers” refers to naturally occurring polymeric materials and/or natural substances that can be polymerized into high molecular weight polymers (Sudesh and Iwata, 2008). Therefore bio based polymers include biopolymers and their associated blends and composites and synthetic polymers made from renewable sources (Sudesh and Iwata, 2008). The term biodegradability refers to natural degradation in the surrounding environment. It should be noted that not all bio based polymers are biodegradable and vice-versa.

Polymeric scaffolds are often designed as temporary structures having the desired physical, chemical, and mechanical properties required for implantation. The use of degradable polymers is desirable because the need for surgical removal is obviated; however, care must be taken to ensure the compatibility of both intermediate and final degradation products, the timing of the degradation process, and how each of these affects the regenerative process. The rate and mechanism of degradation (surface erosion or bulk) will impact the mechanical properties of the scaffold: bulk eroding polymers maintain their physical structure until the molar mass of the polymer is sufficiently low for polymer dissolution in the aqueous surroundings, at which point there is a precipitous loss of mechanical properties; surface eroding polymers lose their shape and mechanical properties gradually over time. For both degradation mechanisms, the regenerative process will inevitably be negatively impacted if the degradation products are toxic to the tissue that has formed and/or if the integrity of the scaffold is lost prior to new tissue formation and integration with the host. This narrows the selection of polymers to those that degrade at rates slow enough for cell integration and tissue growth and to those that produce only biocompatible degradation products (Shoichet, 2009).

The development of synthetic biopolymers has benefited the design and development of three-dimensional (3D) templates or scaffolds that reinforce the tissue and in some cases, organize regenerating tissue for tissue-engineered products (Kim and Mooney, 1998; Mano *et al.*, 1999). Moreover, unlike natural biodegradable polymers, synthetic biopolymers can be easily mass-produced (Middleton and Tipton, 2000). Besides, polymeric scaffolds require high porosity with interconnected pores and desirable chemical properties (Madhally and Matthew, 1999). On the other hand, polymers have undoubtedly improved our lifestyle because

of their wide range of properties available at low cost and hence versatility in applications. It is unacceptable to avoid the use of polymeric materials and hence the need arises for the low cost, renewable resource polymeric materials which can provide the properties of a commodity polymer while minimizing any detrimental effects on the environment.

Biodegradable synthetic polymers (BSPs), such as poly (lactic acids)/ poly(L-lactide) (PLLA) can play a significant role in the commodity area if they possess desired qualities. PLA and its copolymers are part of a diverse group of poly( $\alpha$ -hydroxy acid)s used in biomedical applications since the 1970's. While initially studied for packaging and agricultural applications (Kricheldorf *et al.*, 1996; Sinclair, 1996) these polymers are nowadays mostly used in the biomedical and pharmaceutical industries as controlled drug delivery systems, as well as in the veterinary and agrochemical fields. The aliphatic polyesters such as PLLA are versatile biomaterials due to their biodegradability and biocompatibility (Moon *et al.*, 2000; Moon *et al.*, 2001; Shinoda *et al.*, 2003). PLLA is synthetic biodegradable polymer, which can be used as a pharmaceutical and biomedical material for drug delivery systems and tissue regeneration (Thomson *et al.*, 1995; Ikada and Tsuji, 2000).

The most frequently investigated and widely employed polymer in 3D scaffolds is PLLA (Zhou *et al.*, 2005; Gong *et al.*, 2007; Raghunath *et al.*, 2007; Gui-Bo *et al.*, 2010). PLLA has the advantages of biodegradability, a controllable degradation rate, good mechanical properties and biocompatibility. It can be produced from renewable resources, and it is nontoxic to humans and the environment (Sodergard and Stolt, 2002; Auras *et al.*, 2004). Porous scaffolds of PLLA have been widely used in tissue engineering to guide the regeneration of skin

(Zacchi *et al.*, 1998), bone (Ishaug *et al.*, 1997), cartilage (Li and Tuan, 2005 ) and ligament (Lin *et al.*, 1999).

Several techniques have been reported to produce polymeric porous scaffolds for tissue engineering such as solvent casting, particulate leaching (Reignier and Huneault, 2006), gas foaming (Nam *et al.*, 2000), micro-fabrication, pressure-activated microsyringing (PAM) (Mariani *et al.*, 2006), gravity spinning (Williamson *et al.*, 2006), 3D micro-printing (Hutmacher *et al.*, 2001), electro-spinning (Murphy and Mikos, 2007) and the freeze-extraction method (Ho *et al.*, 2004). Among these techniques, freeze-extraction is the most common, low-cost and high-yield technique with saving time and energy. This method is the easiest technique to scale up synthesising porous scaffolds with interconnected pore networks (Yang *et al.*, 2004). The unique advantage of this method lies in capability of designing 3D nanostructures by well-designed procedure without using any special equipment and porosity of the scaffold can be easily controlled or modified by this method (Ho *et al.*, 2004).

The physical aspects of scaffold design, as with polymer choice, depend largely on the final application. The scaffold is meant to provide the appropriate chemical, physical, and mechanical properties required for cell survival and tissue formation. Essentially, the polymeric scaffold is designed to define the cellular microenvironment (cell niche) required for optimal function (Madlambayan *et al.*, 2005; Madlambayan *et al.*, 2006). Understanding the series of stimuli provided during development and/or healing is the guide to which tissue engineers most often turn when designing a scaffold. Typically, the scaffold is a 3D open-cell, interconnected porous structure, allowing facile communication between the biological cells dispersed in the scaffold. Depending on the intended use, these

structures are also conducive to cell proliferation, migration, and/or differentiation. The stimuli that define the cellular microenvironment include the chemical, physical, and mechanical properties of the scaffold as well as other cells and signaling molecules incorporated into the scaffold design. The 3D of the scaffold is key to its use in tissue engineering, where a 3D cell construct is meant to integrate into a 3D tissue. Determining the appropriate physical structure of the polymeric scaffold requires an understanding of the tissue into which it is being implanted. For example, polymeric scaffolds designed for implantation into the spinal cord have included elaborate designs of the gray and white matter tracts (Moore *et al.*, 2006) while implantations into bone have imitated the porosity of trabecular bone (Holy *et al.*, 2003).

The mechanical properties of the scaffold are dictated by the tissue into which it is implanted. For example, hard tissue, such as bone, necessitates a stiff polymeric scaffold (Ruhé *et al.*, 2005) whereas a soft tissue, such as nerve, requires a malleable polymeric scaffold (Belkas *et al.*, 2005; Katayama *et al.*, 2006; Clements *et al.*, 2009) and an elastomeric tissue, such as skin (or blood vessel), demands a flexible polymeric scaffold (Guan *et al.*, 2005; Guan and Wagner, 2005). In addition to the mechanical properties, the tissue engineered scaffold is designed for enhanced cell penetration and 3-dimensional tissue formation. This has been achieved by incorporating pores or cell-cleavable groups within the scaffold design. For many years, pores were introduced into scaffolds by a variety of processes involving salt leaching (Lu *et al.*, 2000; Lu *et al.*, 2000) phase inversion (Holy *et al.*, 1999; Holy *et al.*, 2000) and high-pressure gasification (Riddle and Mooney, 2004).

Today we understand that the mechanical properties of the scaffold can influence cell proliferation thus attention has refocused on the design of the biomaterial. Most

of the engineered biomaterial scaffolds are polymeric, and thus the opportunity to design polymers for applications in medicine is great. Importantly, our concept of a scaffold includes both the 3-dimensional traditional geometrically defined construct and the newer injectable material, which does not provide a distinct macroscopic architecture but still provides a controlled microenvironment for the cells. It is this microenvironment which is a key determinant of success and is comprised of cell interactions with other cells, soluble or matrix-bound growth factors and adhesion molecules, and the biomaterial itself through mechanical and chemical stimulus. The underlying strategy for the future is to understand the tissue sufficiently to design a polymeric biomaterial with the appropriate properties for success, whether the application is *in vitro* or *in vivo* degradation (Shoichet, 2009).

## **1.2 Problem Statement**

Scaffolds with various porous structures, porosities, pore size and pore interconnectivity can be tailor-made. However, most of the scaffolds have relatively poor mechanical properties and are unable to meet the requirements for certain applications such as tissue engineering, integrity handling, implantation and tissue support during healing (Zhang and Ma, 1999; Zhang and Zhang, 2001; Kothapalli *et al.*, 2005). Hence, there is a need to fabricate 3D polymer scaffolds with improved mechanical properties. (Zhou, Gong *et al.*, 2005). A common method of improving the mechanical properties of a polymer matrix is to incorporate fillers into the polymer as a reinforcement agent. The incorporation of nanometer-sized carbon nanotubes (CNTs) in a polymer matrix leads to remarkably improved properties of the polymer. Multi-walled carbon nanotubes (MWCNTs) are considered to be the ideal reinforcing agent due to their unique properties. CNTs are one of the most

promising candidates for the design of novel polymer composites (Spitalsky *et al.*, 2009). Polymer/CNTs composites could be used as scaffold materials for tissue engineering and bone cell proliferation (Zanello *et al.*, 2006). MWCNTs possess high mechanical strength, thermal conductivity and extraordinary optical properties (Kim *et al.*, 2007). They can be used in the reinforcement of fibers, as atomic force microscopy tips and in nanocomposites as well as in biomedical systems and devices such as sutures, orthopaedic fixation devices and tissue-engineering scaffolds (MacDonald *et al.*, 2005; Abarrategi *et al.*, 2008).

### **1.3 Objectives of research**

The porous structural scaffolds with a suitable pore size, porosity and biodegradability and reinforced mechanical and thermal properties need to be synthesized for tissue engineering applications. Therefore, the objectives of this research were:

- To produce PLLA and PLLA/MWCNT scaffolds by incorporation of MWCNTs into the PLLA as a reinforcement agent.
- To characterize the synthesized PLLA and PLLA/MWCNT scaffolds.
- To study the biodegradability of the PLLA and PLLA/MWCNT scaffolds.
- To optimize the production of the PLA and PLLA/MWCNT scaffolds and evaluate the effect of different parameters using response surface methodology (RSM) by design of experiment (DOE) software.

## **1.4 Outline of the thesis**

This thesis is organized into five chapters:

**Chapter 1**, commenced with some basic information on the definition of biomaterials, biodegradable polymers and MWCNTs followed by a brief introduction on the overview of the biodegradable polymers application in tissue engineering. The concerned issues, which generated the ideas and inputs for this research work, were also elaborated upon. The primary objectives and the general flow of the research program were also outlined.

**Chapter 2**, relates some background and classification on engineering polymeric biomaterials for biomedical applications and tissue engineering. Explications on the functions, requirements and available synthesis methods of scaffolds production with special focus on the interpenetrating PLLA as biodegradable polymer with MWCNTs by freeze extraction method and the applications of resulted scaffolds were also provided. Subsequently, a literature review was done on various published works on PLLA and MWCNTs based composite biomaterials and scaffolds for tissue engineering and biomedical applications particularly those that are closely related to this work. Finally we have discussed about some statistical optimization methods which has been used in this work.

**Chapter 3**, details the experimental procedures employed in this research. Descriptions of lab equipments used as well as any other processing techniques utilized in generating any data that were used and presented in the research are reported.

**Chapter 4**, is actually the results and discussion chapter according to the research objectives. This chapter describes the synthesis and characterization of PLLA and PLLA/MWCNT porous scaffolds prepared by the freeze-extraction method. In addition, investigates the optimum condition of scaffolds production based on DOE and finally in vitro degradation studies of the scaffolds were assessed by immersing the scaffolds in phosphate buffered saline (PBS) for up to 24 weeks.

**Chapter 5**, provides a summary of the results obtained in this research and presents concluding remarks on the present work and also recommendations for future studies.

## CHAPTER 2

### LITERATURE REVIEW

#### 2.1 Polylactide/poly(lactic acid)

##### 2.1.1 Introduction

PLA obtained from L- and D-lactides is semi-crystalline (0-37%) and a relatively hard material with melting temperatures ranging from 170-190 °C and glass transition temperatures ( $T_g$ ) ranging from 50-65 °C (Tsuji *et al.*, 2002). The melting temperatures can be as high as 220 °C and as low as 130 °C depending on the distribution of L- and D-lactides in the backbone (Farrington *et al.*, 2005). Witzke *et al.* reported that the melting temperatures decrease by 3°C for every 1% initial *meso*lactide concentration and almost no crystallinity with 18% *meso*-lactide (Witzke, 1997). PLA has relatively low thermal stability and above 190 °C, the molar weight decreases and thermal degradation (weight loss) can be observed in the range of 235-255 °C (Engelberg and Kohn, 1991) Because of the semi-crystalline nature of PLA, physical properties such as changes in the crystalline/amorphous ratio are strongly affected by the thermal effects (Celli and Scandola, 1992). The heat of fusion for 100% crystalline PLA from L-lactides ranges from 93-203 J/g as reported in different researches as listed in Table 2.1. Crystallization of PLA has been thoroughly investigated such as by Fischer *et al.* (Fischer *et al.*, 1973) about melt and solution crystallization, Kalb and Pennings (Kalb and Pennings, 1980) about spherulitic growth from melt, Vasanthakumari and Pennings (Vasanthakumari and Pennings, 1983) about crystallization kinetics and crystal growth, Cohn *et al.* (Cohn *et al.*, 1987) about amorphous/crystalline morphology and Kishore *et al.* (Kishore *et al.*, 1984) about isothermal melt mechanism. Upon heating amorphous samples,

crystallization rates increase with an increase in temperature (100 -160 °C) and reach a maximum before showing a decreasing trend (Tsuji *et al.*, 2005).

Table 2. 1 Thermal properties of PLA(Jamshidi *et al.*, 1988; Ikada and Tsuji, 2000; Tsuji, Miyase *et al.*, 2005)

<b>Properties</b>	<b>Value</b>	<b>Units</b>
Degree of crystallinity, XC	0-37	%
Melting temperature, Tm	170-190	°C
Equilibrium melting temperature, Tm°	205-215	°C
Heat of fusion for 100% crystalline PLLA	93-203	J/g
Glass transition temperature, Tg	50-65	°C
Decomposition temperature, Td	235-255	°C

The crystallization is strongly affected by the optical purity of PLA. The crystallization time for PLLA increased 40% with the incorporation of 1% meso-lactide (Kolstad, 1996). Iannace and Nicolais reported a maximum crystallization rate at 105 °C and the overall rate of bulk crystallization (Iannace and Nicolais, 1997). According to the rate that the chains are deposited on the crystal surface, Hoffman divided the melt crystallization kinetics in three regimes (Sperling, 1986). As the temperature is lowered through regimes A, B, and C, the crystallization rate becomes larger than the nucleation rate. In PLA, the transition of crystallization kinetics from regime B to regime A was observed above 163 °C by Vasanthakumari and Pennings whereas the transition of crystallization kinetics from regime C to regime B was observed around 115 °C by Iannace and Nicolais (Iannace and Nicolais, 1997). Di Lorenzo reported the transition of the crystallization kinetics from regime C to regime B at 120 °C by the Hoffman and Lauritzen theory. Spherulitic growth rate was found to be function of crystallization temperature and molecular weight (Vasanthakumari and Pennings, 1983). Growth rate (G) was

observed to increase with a decrease in molecular weight. According to Vasanthakumari and Pennings, a viscosity-average molecular weight change from 150,000 g/mol to 690,000 g/mol reduces the growth rate from 5  $\mu\text{m}/\text{min}$  to 2.5  $\mu\text{m}/\text{min}$  (Vasanthakumari and Pennings, 1983) Di Lorenzo and He et al. reported the growth rate of 6.7 and 9.1  $\mu\text{m}/\text{min}$ , respectively for PLA isothermally crystallized at 130 °C (Di Lorenzo, 2001).

### 2.1.3.2 Physical Properties of PLA

The important physical properties of PLA are summarized in Table 2.2. The density of PLA was reported to be in the range of 1.25 to 1.29  $\text{g}/\text{cm}^3$  and the refractive index between 1.35-1.45 (Tsuji, 2005). Solubility parameter ( $\delta$ ) of PLA was reported in the range of 19.0-20.5 ( $\text{J}/\text{cm}^3$ )<sup>0.5</sup> and PLA is reported to be soluble in dioxane, chloroform, methylene chloride, dichloroacetic acid, and acetonitrile (Kharas *et al.*, 1994). Crystalline PLA is not soluble in tetrahydrofuran, ethyl acetate, or acetone. PLA is insoluble in water, alcohols and alkanes and hence precipitate in alcohols and alkanes. The reported surface energy of PLA ranges from 35.9-43.9 mN/m depending on the processing and detailed information can be found in the literature (Biresaw and Carriere, 2002). The permeability of PLA is an important factor for its packaging applications and depends on the crystalline/amorphous phase distribution as reported by (Shogren *et al.*, 1997) however, other common polymers such as polyethylene terephthalate and polypropylene have very low permeabilities (<1.3  $\text{g}/\text{m}^2/\text{day}$  ).

Table 2. 2 Physical properties of PLA (Shogren, 1997; Tsuji and Muramatsu, 2001; Biresaw and Carriere, 2002)

Property	Value	Units
----------	-------	-------

Density	1.25-1.29	g/cm <sup>3</sup>
Refractive index (fiber)	1.35-1.45	
Solubility parameter ( $\delta$ )	19-20.5	(J/cm <sup>3</sup> ) <sup>0.5</sup>
Surface energy	35.9-43.9	mN/m
Permeability at 25 °C (Amorphous PLA)	172	g/m <sup>2</sup> /day
Permeability at 25 °C (Crystalline PLA)	82	g/m <sup>2</sup> /day

## 2.1.4 PLA Modifications

### 2.1.4.1 Copolymerization

One of the important and most utilized methods of PLA modification is copolymerization which results in a product that has combined effects of two or more polymers. Copolymers of PLA with various architectures such as block (Kataoka *et al.*, 2001) random (Baratian *et al.*, 2001) alternating (Bechtold *et al.*, 2001) graft (Cai *et al.*, 2003; Wu *et al.*, 2005) and hyperbranched (Gottschalk and Frey, 2006; Pitet *et al.*, 2007) have been reported. Polymerizations of L-lactide with other lactides and other polymer precursors result in copolymers with modified properties of PLA. The random copolymerization of L-lactide with small amounts of D-lactide reduces crystallinity as well as the substantially reducing the spherulitic growth rates (Baratian, Hall *et al.*, 2001). The crystallization and microstructure of copolymers of L-lactides with *meso*-lactides have been reported by Huang *et al.* (Huang *et al.*, 1998). Copolymers of PLA with numerous polymers such as polyglycolide (PGA) (Min *et al.*, 2005) poly( $\epsilon$ -caprolactone) (PCL) (Li *et al.*, 2002) polyisoprene (Schmidt and Hillmyer, 1999) polystyrene (PS) (Zalusky *et al.*, 2002) polyethylene (PE) (Wang and Hillmyer, 2001) polypropylene (PP), poly(ethylene glycol) (PEG), poly(ethylene oxide) (PEO) (Du *et al.*, 1995; Li *et al.*, 2005) and poly(methyl methacrylate) (PMMA) (Gautier *et al.*, 2001) have been reported and produced with

varying desired properties. The copolymers of glycolide with lactides are particularly reviewed by Tirelli et al. (Tirelli, 2006) and have applications in the medical and pharmaceutical fields. For highly crystallizable and hydrolytically stable PLA, Abayasinghe and coworkers (Abayasinghe *et al.*, 2005) synthesized oligoethylene-end-capped PLA using hydroxy-terminated oligoethylene as macroinitiators for the ROP of L-lactide as shown in Figure 2.9. Haynes et al. (Haynes *et al.*, 2007) used hydroxy-terminated perfluoropolyether as the macroinitiator for the ROP of L-lactide resulting in a very low surface energy PLA based copolymer with a water contact angle above 100°. At the other extreme, PLA was made more hydrophilic, flexible and biodegradable by copolymerization with poly(ethylene oxide)/poly(ethylene glycol) (Lemmouchi *et al.*, 2007) In addition to linear copolymers, PLA has been modified as graft copolymers, branched copolymers, and cross-linked polymers (Kitamura and Matsumoto, 2007).

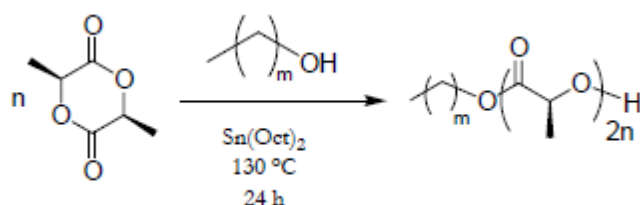


Figure 2. 1 Synthesis of oligoethylene-end-capped PLA

Terpolymerization of equimolar ratios of L-lactide, diglycidyl ether of bisphenol A (DGEBA), and the 4,4'-hexafluoroisopropylidenediphenol (6F-Bis-A), catalyzed by 18-crown-6-ether and potassium chloride, resulted in an amorphous terpolymer with a glass transition of 80 °C as reported by Abayasinghe and Smith (Abayasinghe and Smith Jr, 2003). Smith and co-workers reported (PLA)-*block*-poly(hydroxyalkanoate (PHA) block copolymers by ring-opening polymerization of L-lactide using PHA as macro-initiator in presence of (Sn(Oct)<sub>2</sub>) (Haynes *et al.*, 2007). They also reported poly(ester amide) random copolymers by ring opening

polymerization of L-lactide and novel depsipeptide monomer, 6,6'-dimethyl-2,5-morpholinedione, in presence of  $(\text{Sn}(\text{Oct})_2)$  (Abayasinghe *et al.*, 2004).

#### **2.1.4.2 PLA Blending**

Blending provides an alternative modification route to copolymerization and is often less expensive. PLA has been blended with numerous polymeric materials to improve its physical properties, hydrolytic stability, degradation and hydrophilic properties. Blends of PLA with PE (Anderson *et al.*, 2003), PS (Sarazin and Favis, 2003), PMMA (Eguiburu *et al.*, 1998), poly(sebacic anhydride), polysaccharide (Dubois and Narayan, 2003) poly(vinylpyrrolidone) (Zhang *et al.*, 2003), polyurethane, poly(dimethyl siloxane) (Lee *et al.*, 2006), chitosan (Peesan *et al.*, 2005; Wan *et al.*, 2006) and poly(vinylalcohol), have been reported. Wan *et al.*, (2006) prepared biodegradable blend membranes by blending PLA with chitosan using solvent-casting and solvent-extraction processing techniques and found a significant influence of processing conditions on the morphology. Interfacial properties of blends are important factors for a successful blend material and Biresaw and Carriere (Biresaw and Carriere, 2002) measured the interfacial tension of PLA/PS blends at 170-200 °C by an embedded fiber retraction method and reported a value of  $5.4 \pm 1.3$  mN/m. Wu and Liao compared the blend properties of hyaluronic acid with PLA and acrylic acid grafted PLA(PLA-*co*-AA) and reported higher melting temperatures and improved tensile strengths for the PLA-*co*-AA blends in comparison to PLA blends (Wu and Liao, 2005).

### 2.1.5 Degradation

All polymers degrade but it is the degradation rate which classifies polymers as degradable (degrades during or immediately after their application) and nondegradable (degrades after substantially longer time than the duration of their application) polymers (Göpferich, 1996). Polymers can degrade by any combination of various degradation mechanisms including photo degradation by radiation, thermal degradation by heat, mechanical degradation by application of stress and degradation by chemical agents. Aliphatic biodegradable polymers are susceptible to hydrolysis and biodegradation. Degradation is defined as a chemical phenomenon in which the polymer chains are converted to oligomers and also oligomers to monomers by bond cleavage. Erosion is defined as a physical phenomenon which results in the depletion of material by dissolution and diffusion and is classified mainly into bulk and surface erosion (Tamada and Langer, 1993). For bulk erosion, material is lost from the entire volume and degradation rate decreases as the amount of material decreases, whereas, for surface erosion, the loss of material is from the surface of the specimen and thus the rate is proportional to the surface area. Core-accelerated bulk erosion is possible for the thicker polymer samples where low molecular weight degradation products are trapped inside the core of the sample and therefore accelerate degradation. A schematic for bulk, surface and core-accelerated bulk erosion are compared in Figure 2.10. Polymer degradation is affected by numerous material and hydrolysis media factors such as bond stability (amides>esters>ortho>esters>anhydrides), hydrophobicity, water diffusivity, steric effects, microstructure (crystallinity/porosity), pH and temperature of hydrolysis media, effect of degraded products and polymer chain length (Gopferich and Langer, 1993; Göpferich, 1996).

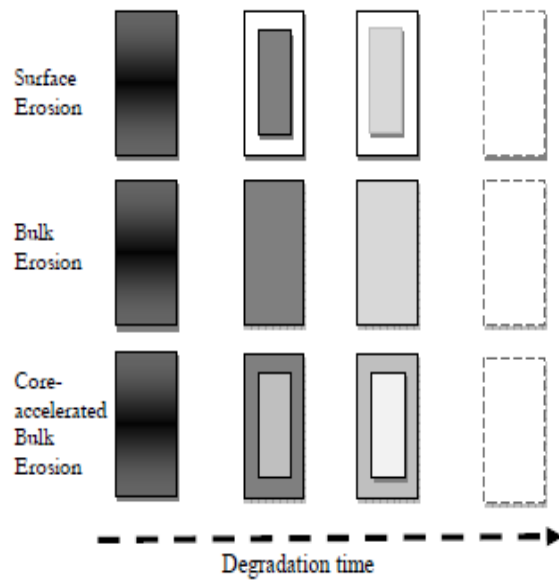


Figure 2. 2 Hydrolysis mechanism for PLA [1]

### 2.1.6 PLA applications

PLA and its copolymers have been increasingly studied and utilized in the biomedical fields for medical applications such as skin, cartilage, blood vessel (Shoichet, 2009), sutures, drug delivery and scaffolds for tissue engineering (Tsuji, 2005).

Table 2. 3 Applications of PLA and their copolymer (Ikada and Tsuji, 2000)

<b>Function</b>	<b>Purpose</b>	<b>Examples</b>
Bonding	Suturing	Vascular and intestinal anastomosis
	Fixation	Fractured bone fixation
	Adhesion	Surgical adhesion
Closure	Covering	Wound cover, local hemostasis
	Occlusion	Vascular embolization
Separation	Isolation	Organ protection
	Contact inhibition	Adhesion prevention

Scaffold	Cellular proliferation Tissue guide	Skin reconstruction, blood vessel reconstruction Nerve reunion
Capsulation	Controlled drug delivery	Sustained drug release
Industrial applications	Agriculture, forestry	Mulch films, temporary replanting pots, delivery and system for fertilizers and pesticides
	Fisheries	Fishing lines and nets, fishhooks
Composting	Civil engineering and construction industry Outdoor sports	Forms, vegetation nets and sheets, water-retention sheets Golf tees, disposable plates, cups, bags, and cutlery
	Food package	Package, containers, wrappings,  bottles, bags, films, retail bags, six-pack rings
	Toiletry	Diapers, feminine hygiene products
	Daily necessities	Refuge bags, cups

---

Recent technological advances in the production of lactic acid have made PLA shift from a high price to high volume commodity polymer that could be seen as a substitute to PBPs. Excellent barrier properties for flavor constituents and heat sealability of the biaxially-oriented PLA films makes it ideal for food packaging applications (Smith *et al.*, 2001). Some of the important applications of PLA and its copolymers are listed in Table 2.3.

In addition to the applications mentioned in Table 2.3, PLA polymer has been evaluated for a range of applications in the packaging, films, and fiber areas and these are listed segment-wise in detail in Table 2.4. In the future, a reduction in price, sustainability due to renewable raw materials, and also the positive environmental aspects of PLA could probably make it a potential commodity polymer.

Table 2. 4 Commercial applications of PLA (Ikada and Tsuji, 2000)

Segments	Commercially available applications
Segments	Commercially available applications
Rigid thermoforms	Clear short shelf-life trays and lids, opaque dairy containers, consumer displays and electronics packaging, disposable articles, cold drink cups
Biaxially-oriented films	Shrink wrap for consumer goods packaging, twist wrap candy and flower wrap, windows for envelopes, bags and cartons
Bottles	Short shelf-life milk and oil packaging
Apparel	Sport, active and underwear, fashion
Non-wovens	Agricultural and geo textiles, hygiene products, wipes, shoe liners
Household, industrial, and institutional fabrics	Bedding, drapery, table cloths, curtains, mattress ticking, wall and cubicle fabrics, upholstery
Carpet	Surface yarn and fibers
Fiberfill	Pillows, comforters, mattresses, duvets
Foams	Structural protective foams

## 2.2 Carbon nanotubes (CNTs)

### 2.2.1 Synthesis of CNTs

There has been remarkable effort and interest for the growth improvement and optimization of the CNTs. Synthesis of CNTs with desired configurations and structural characteristic has been vastly investigated during the last decade and yet no full control over the geometry, purity, and properties of the synthesized CNTs has been obtained (Ebbesen and Ajayan, 1992; Osman and Srivastava, 2001; Baughman *et al.*, 2002; Ajayan *et al.*, 2003; Fa *et al.*, 2004; Wang *et al.*, 2007). CNTs are long cylinders of covalently bonded carbon atoms. The ends of the cylinders may or may not be capped by hemifullerenes. There are two basic types of CNT: single-wall carbon nanotubes (SWCNT) and multiwall carbon nanotubes (MWCNT). SWNT can be considered as a single graphene sheet (graphene is a monolayer of  $sp^2$ -bonded

carbon atoms) rolled into a seamless cylinder. The carbon atoms in the cylinder have partial  $sp^3$  character that increases as the radius of curvature of the cylinder decreases. MWCNT consist of nested graphene cylinders coaxially arranged around a central hollow core with interlayer separations of  $\sim 0.34$  nm, indicative of the interplane spacing of graphite (Saari and Konttinen, 1989). A special case of MWCNT is double-wall nanotubes (DWCNT) that consist of two concentric graphene cylinders. DWCNT are expected to exhibit higher flexural modulus than SWCNT due to the two walls and higher toughness than regular MWCNT due to their smaller size (Nakamura *et al.*, 2004). The nanotubes can be filled with foreign elements or compounds, e.g., with  $C_{60}$  molecules, to produce hybrid nanomaterials which possess unique intrinsic properties, such as transport properties (Nakamura, Yokohama *et al.*, 2004). These hybrid nanomaterials currently have limited availability, but as production increases this might be a new opportunity for polymer nanocomposites.

The different ways of rolling graphene into tubes are described by the tube chirality (or helicity or wrapping) as defined by the circumferential vector,  $C^*_h = na^*_1 + ma^*_2$  have shown in Figure 2.11, where the integers ( $n, m$ ) are the number of steps along the unit vectors ( $a^*_1$  and  $a^*_2$ ) of the hexagonal lattice (Gupta *et al.*, 2006). Using this ( $n, m$ ) naming scheme, the three types of orientation of the carbon atoms around the nanotube circumference are specified as arm chair ( $n = m$ ), zigzag ( $n = 0$  or  $m = 0$ ), or chiral (all others). The chirality of nanotubes has significant impact on its transport properties, particularly the electronic properties. All armchairs SWCNT are metallic with a band gap of 0 eV. SWCNT with  $n - m = 3i$  ( $i$  being an integer and  $\neq 0$ ) are semimetallic with a band gap on the order of a few meV, while SWCNT with  $n - m \neq 3i$  are semiconductors with a band gap of ca. 0.5–1 eV (Ueda

and Tabata, 2003). Each MWCNT contains a variety of tube chiralities, so their physical properties are more complicated to predict.

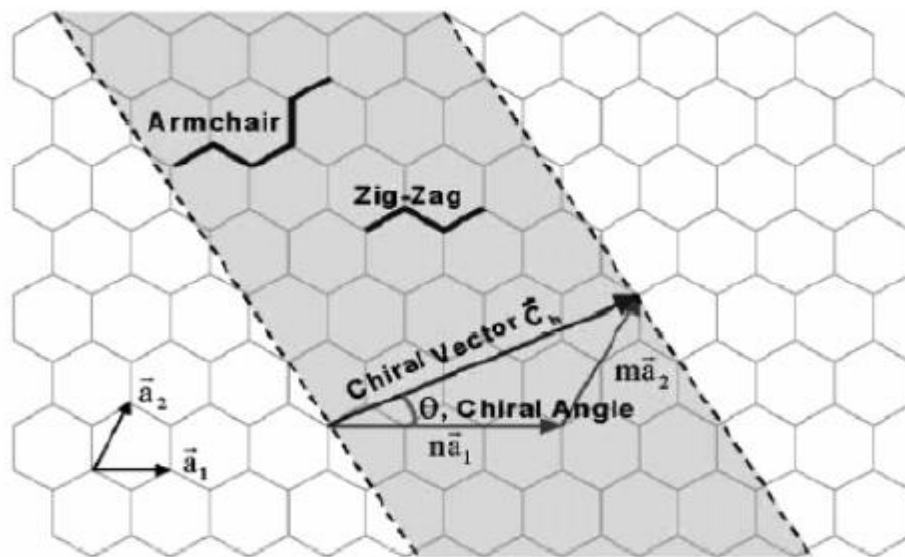


Figure 2. 3 Schematic diagram showing how a hexagonal sheet of graphene is “rolled” to form a CNTs

Presently, MWCNT and SWCNT are mainly produced by three techniques: arc discharge, laser ablation, and chemical vapor decomposition (CVD). A number of reviews (Saari and Kontinen, 1989; Gupta, Tator et al., 2006) are available on these production techniques. Each of these growth techniques has unique advantages and disadvantages. Based on the requirements for the properties and structural characteristics of CNTs for specific applications a proper growth technique has to be identified and used. Arc discharge and laser ablation methods involve the condensation of hot gaseous carbon atoms generated from the evaporation of solid carbon. In CVD a gaseous carbon source (hydrocarbon, CO) is decomposed catalytically, and the nanotubes are deposited on a substrate or grow from a substrate. If CNTs are required to be grown and aligned in a specific pattern and direction for a certain application then CVD technique has to be used. Compared with arc and laser methods, CVD might offer more control over the length and structure of the

produced nanotubes, and the process appears scalable to industrial quantities. Carbon Nanotechnology Inc. (Houston, TX) produces SWNT using a floating catalyst CVD method, known as high-pressure catalytic decomposition of carbon monoxide or HiPco.

It should be mentioned that CNTs have tendency to grow only on certain types of substrate materials and the growth quality and CNTs alignments greatly depends on the employed processing technique and growth parameters such as; atmospheric condition, type and size of catalyst particles, material of the substrate, doped material, carrier gas, and the carbon source. All known preparations of CNT give mixtures of nanotube chiralities, diameters, and lengths along with different amount and type of impurities. This CNT heterogeneity has important implications when purifying carbon nanotubes and preparing nanotube/polymer composites. For example, smaller diameters SWNT are more susceptible to both thermal degradation and chemical functionalization, such that the diameter distribution can be altered between SWNT synthesis and nanotube/polymer composite fabrication. A typical SWNT average diameter is  $\sim 1.2\text{--}1.4$  nm, and the minimum diameter of a stable free-standing SWNT is limited by curvature induced strain to  $\sim 0.4$  nm (Lavik *et al.*, 2005). The variation in SWNT diameter is also illustrated by the coexistence of various wrappings ( $n, m$ ), where the circumferential vectors are used to calculate the nanotube diameters. MWNT can have diameters from several nanometers to several hundred nanometers. The reported lengths of nanotubes range from several tens of nanometers to several centimeters (Shea *et al.*, 2000). The properties of the nanotube/polymer composites will vary significantly depending on the distribution of the type, diameter, and length of the nanotubes.

### 2.2.2 Mechanical Properties of CNTs

The potential use of individual CNTs as nanomaterials/devices warrants detailed investigations of their mechanical behavior based on structural and geometrical configurations. There have been many applications proposed for CNTs such as high-strength nanocomposites, sensors, actuators, storage systems, filters, carriers, nanometer-sized semiconductor and superconductor devices, and in general nano-electromechanical devices and systems. CNTs exhibit remarkable mechanical properties significantly different from other engineering materials (Treacy *et al.*, 1996; Baughman, Zakhidov *et al.*, 2002; Ratner and Ratner, 2002; Goddard, 2007). The Young's modulus of the CNTs is very large in the axial direction and yet they are very flexible because of the relatively large (length/diameter) ratio (Ratner and Ratner, 2002; Goddard, 2007). Therefore, due to their high stiffness, high strength, and low weight, CNTs could also be excellent candidates for structural applications, especially for high performance composite materials. The effectiveness of modeling and predicting the nanotube and nanocomposites properties have been demonstrated by many previous works (Sinnott *et al.*, 1998). Krishnan *et al.* (Krishnan *et al.*, 1998) have estimated the Young's modulus of a SWCNT to be 1.25 TPa by observing their freestanding room-temperature vibrations in a transmission electron microscope. Liu (Lu, 1997) investigated the elastic properties of CNTs and nanoropes using an empirical force constant model and reported the Young's modulus of CNT (~ 1 TPa) and shear modulus (~ 0.5 TPa). An experimental study conducted by Cao *et al.* (Cao *et al.*, 2005) reported the Young's modulus of CNTs as 1.8 TPa. Ozaki *et al.* (Ozaki *et al.*, 2000) investigated the elastic properties of graphite sheet using a simple harmonic potential and an analytic bond-order potential. They suggested that the unique elastic properties of CNTs originate from those of a six-membered ring. Harik

(Liang and Xu, 2003) analyzed the validity of continuum beam theory for the constitutive behavior of CNTs and other nano-rods of non-carbon materials.

The effects of chirality of CNTs on their properties have been a topic of interest in recent years. Using an empirical force-constant model, Lu (Lu, 1997) has reported that for SWCNTs, the elastic modulus does not depend on geometry or the chirality of the nanotubes. Liang et al. (Liang and Xu, 2003) have studied the chirality effect of an open end SWCNT on field emission and reported that the characteristic of the emission-current line density versus field was dependent on the chirality of nanotubes. Kristic et al. (Krsti *et al.*, 2004) reported that due to their chiral character, the mechanical behavior of chiral nanotubes in a magnetic field differ from their achiral counterparts. Based on several previously published theoretical and experimental works a value of nearly 1 TPa and 63 GPa are well agreed for the axial Young's modulus and axial tensile strength of CNTs (Treacy, Ebbesen et al., 1996; Krishnan, Dujardin et al., 1998; Van Lier *et al.*, 2000; Li and Chou, 2003).

Even though many attempts are made to experimentally and theoretically investigate the longitudinal mechanical properties of CNTs, inadequate studies have been performed for the prediction of CNTs radial (or transverse) mechanical properties. Palaci et al. (Palaci *et al.*, 2005) used atomic force microscopy and molecular dynamics simulation to experimentally and theoretically study the radial elasticity of the MWCNTs. They have reported that the radial Young's modulus strongly depends on the radius of CNTs and it reaches an asymptotic value of  $30 \pm 10$  GPa for CNTs with external radii of less than 5 nm. Shen et al. (Shen *et al.*, 2000) studied the radial compression of the multi-walled CNTs under an asymmetric stress using a scanning probe microscope with an indentation/scratch function. They have